

# UC Irvine

## UC Irvine Previously Published Works

### Title

$\alpha$ -Methylation Enables the X-ray Crystallographic Observation of Oligomeric Assemblies Formed by a  $\beta$ -Hairpin Peptide Derived from A $\beta$ .

### Permalink

<https://escholarship.org/uc/item/5jj1c5bp>

### Authors

Samdin, Tuan  
Kreutzer, Adam  
Sahrai, Victoria  
et al.

### Publication Date

2024-12-17

### DOI

10.1021/acs.joc.4c02344

Peer reviewed

# $\alpha$ -Methylation Enables the X-ray Crystallographic Observation of Oligomeric Assemblies Formed by a $\beta$ -Hairpin Peptide Derived from $A\beta$

Tuan D. Samdin, Adam G. Kreutzer, Victoria Sahrai, Michał Wierzbicki, and James S. Nowick\*



Cite This: *J. Org. Chem.* 2025, 90, 394–400



Read Online

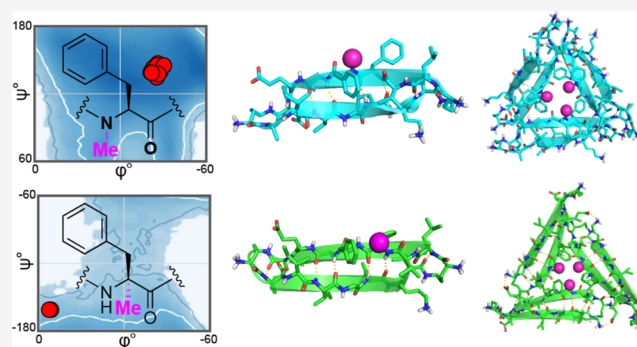
ACCESS |

Metrics & More

Article Recommendations

Supporting Information

**ABSTRACT:** The assembly of the  $\beta$ -amyloid peptide  $A\beta$  into toxic oligomers plays a significant role in the neurodegeneration associated with the pathogenesis of Alzheimer's disease. Our laboratory has developed  $N$ -methylation as a tool to enable X-ray crystallographic studies of oligomers formed by macrocyclic  $\beta$ -hairpin peptides derived from  $A\beta$ . In this investigation, we set out to determine whether  $\alpha$ -methylation could be used as an alternative to  $N$ -methylation in studying the oligomerization of a  $\beta$ -hairpin peptide derived from  $A\beta$ .  $\alpha$ -Methylation permits the crystallographic assembly of a triangular trimer and ball-shaped dodecamer, resembling assemblies formed by the  $N$ -methylated homolog. Subtle differences are observed in the conformation of the  $\alpha$ -methylated peptide when compared to the  $N$ -methylated homolog. Notably,  $\alpha$ -methylation appears to promote a flatter and more extended  $\beta$ -sheet conformation than that of  $N$ -methylated  $\beta$ -sheets or a typical unmodified  $\beta$ -sheet.  $\alpha$ -Methylation provides an alternative to  $N$ -methylation in X-ray crystallographic studies of oligomers formed by peptides derived from  $A\beta$ , with the attractive feature of preserving NH hydrogen-bond donors along the peptide backbone.



## INTRODUCTION

Oligomers formed by the  $\beta$ -amyloid peptide  $A\beta$  are thought to play a central role in Alzheimer's disease.<sup>1–4</sup> Our understanding of the relationship between  $A\beta$  oligomers and their biological activity in the Alzheimer's brain, however, is limited by the absence of any high resolution structures of endogenous  $A\beta$  oligomers. Efforts to study native  $A\beta$  oligomers at high-resolution are frustrated by the heterogeneous, metastable, and polydisperse nature of these assemblies, and the preference of  $A\beta$  to form insoluble fibrillar aggregates instead.<sup>5–8</sup> Chemical and *in silico* models of  $A\beta$  oligomers have thus emerged as useful tools in approximating the structures of endogenous oligomers. The assemblies formed by these model systems highlight the importance of edge-to-edge backbone hydrogen bonding in determining the structure and stoichiometry of  $A\beta$  oligomers.<sup>9–13</sup>

Solution-phase NMR studies by Olejniczak,<sup>9</sup> Hård and Hoyer,<sup>10</sup> and Ciudad<sup>12</sup> have identified  $A\beta$   $\beta$ -hairpins as an important structural element of  $A\beta$  oligomers.<sup>14</sup> To gain insight into potential structures of native  $A\beta$  oligomers, the Nowick laboratory has developed macrocyclic  $\beta$ -hairpin peptides as synthetic mimics of  $A\beta$   $\beta$ -hairpins. Many of these macrocyclic  $\beta$ -hairpin peptides comprise two  $A\beta$  derived heptapeptide  $\beta$ -strand segments linked by two  $\delta$ -linked ornithine ( $\delta$ Orn) turn units that constrain the peptide to a

macrocycle (Figure 1).<sup>15,16</sup> These macrocyclic  $\beta$ -hairpin peptides can assemble to form well-defined oligomers in the crystal state, allowing our laboratory to study the assembly of different  $A\beta$ -derived  $\beta$ -hairpins at atomic-level detail using X-ray crystallography. These studies have revealed a plethora of  $A\beta$  oligomer models that differ in stoichiometry and structure.<sup>17–26</sup>

To prevent uncontrolled aggregation of these  $A\beta$ -derived  $\beta$ -hairpin peptides, we typically incorporate an  $N$ -methyl amino acid on one strand of the macrocycle. Backbone  $N$ -methylation controls assembly of the  $A\beta$   $\beta$ -hairpin model system by preventing fibril formation, enabling crystallization, and thus the observation of crystallographic oligomers. X-ray crystallographic studies of oligomers formed by these  $A\beta$  derived macrocyclic  $\beta$ -hairpin peptides have revealed the formation of dimers and trimers that further assemble to form tetramers, hexamers, octamers, and dodecamers.<sup>16</sup> Peptide **1**<sub>F20(N-Me)</sub> illustrates a representative  $N$ -methylated macrocyclic  $\beta$ -hairpin

**Received:** September 19, 2024

**Revised:** December 4, 2024

**Accepted:** December 10, 2024

**Published:** December 17, 2024



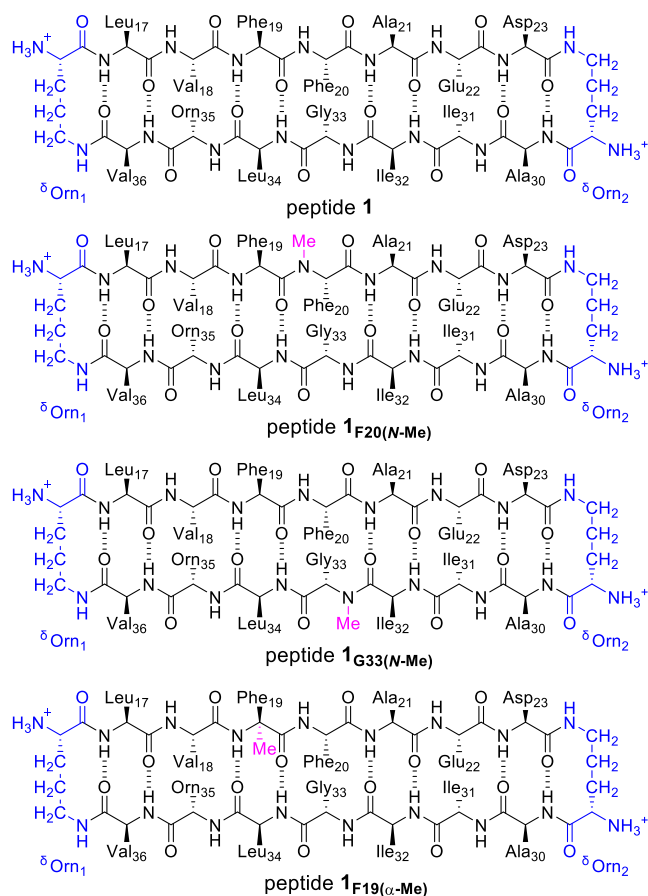


**Figure 1.** Chemical structures of macrocyclic  $\beta$ -hairpin peptides **1**<sub>F20(N-Me)</sub>, **1**<sub>G33(N-Me)</sub>, **1**, and **1**<sub>F19( $\alpha$ -Me)</sub>.  $\delta$ Orn turn units are shown in blue and methyl groups are shown in magenta. Peptide **1**<sub>F20(N-Me)</sub> is an analog of peptide **1** with an *N*-methyl group on Phe<sub>20</sub>. Peptide **1**<sub>G33(N-Me)</sub> is an analog of peptide **1** with an *N*-methyl group on Gly<sub>33</sub>. Peptide **1**<sub>F19( $\alpha$ -Me)</sub> is an analog of peptide **1** with a *C* $\alpha$ -methyl group on Phe<sub>19</sub>.

peptide that we have studied (Figure 1).<sup>17</sup> Peptide **1**<sub>F20(N-Me)</sub> contains two  $\beta$ -strands comprising *A* $\beta$  residues 17–23 and 30–36, two  $\delta$ Orn turn units that constrain the peptide to a macrocycle, and an *N*-methyl group on Phe<sub>20</sub>. To improve solubility, Met<sub>35</sub> is replaced by an  $\alpha$ -linked Orn. X-ray crystallography reveals that three monomers of peptide **1**<sub>F20(N-Me)</sub> assemble to form a triangular trimer (Figure 2a). Hydrophobic side chain packing and intermolecular hydrogen-bonding interactions between the backbone amides of the  $\beta$ -strands containing *A* $\beta$ <sub>17–23</sub> drive assembly and stabilize the triangular trimer.

To probe the role of the *N*-methyl group in directing the assembly of the triangular trimer formed by peptide **1**<sub>F20(N-Me)</sub>, our laboratory also studied peptide **1**<sub>G33(N-Me)</sub>.<sup>17</sup> Peptide **1**<sub>G33(N-Me)</sub> is a homolog of peptide **1**<sub>F20(N-Me)</sub>, in which the *N*-methyl group is on Gly<sub>33</sub> instead of Phe<sub>20</sub> (Figure 1). X-ray crystallographic studies of peptide **1**<sub>G33(N-Me)</sub> revealed the formation of a nearly identical triangular trimer to the one formed by peptide **1**<sub>F20(N-Me)</sub> (Figure 2b). The triangular trimers formed by peptide **1**<sub>F20(N-Me)</sub> and peptide **1**<sub>G33(N-Me)</sub> primarily differ in how each assembly accommodates the *N*-methyl group. In the trimer formed by peptide **1**<sub>F20(N-Me)</sub> the *N*-methyl groups project inward, toward the center of the trimer, and prevent the formation of three intermolecular

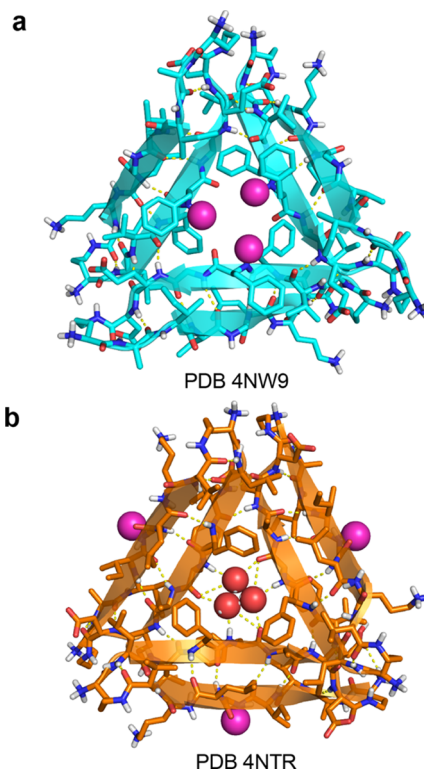


**Figure 2.** X-ray crystallographic structures of triangular trimers formed by *N*-methylated macrocyclic  $\beta$ -hairpin peptides (a) **1**<sub>F20(N-Me)</sub> and (b) **1**<sub>G33(N-Me)</sub>. *N*-Methyl groups are represented as magenta spheres. Ordered water is represented as red spheres.

backbone hydrogen bonds. In the trimer formed by peptide **1**<sub>G33(N-Me)</sub> the *N*-methyl groups project outward, away from the center of the trimer, and allow the backbone amide groups of Phe<sub>20</sub> to coordinate three ordered water molecules.

Although the location of the *N*-methyl group does not affect the crystallographic assembly of a triangular trimer formed by peptide **1**<sub>F20(N-Me)</sub> or peptide **1**<sub>G33(N-Me)</sub>, its presence does remove an NH hydrogen-bond donor from each monomer in the trimer. Interactions at the hydrogen-bonding edges of  $\beta$ -hairpins may have a significant role in directing *A* $\beta$  oligomer stoichiometry and conformation. Restoring the hydrogen-bonding interactions lost by incorporation of an *N*-methyl group may allow the assembly of a macrocyclic  $\beta$ -hairpin peptide derived from *A* $\beta$  to better mimic endogenous *A* $\beta$  oligomers.

Here, we set out to modify the design of a macrocyclic  $\beta$ -hairpin peptide derived from *A* $\beta$ <sub>17–36</sub> to permit additional hydrogen bonding interactions that are lost by *N*-methylation. We initially attempted to remove the methyl group entirely, furnishing peptide **1** (Figure 1). Peptide **1** did not form crystals and instead formed precipitates without any obvious crystalline structure in the conditions screened, thus precluding characterization by X-ray crystallography. To block aggregation, permit the formation of crystals suitable for X-ray crystallography, and allow all backbone NH groups to participate in hydrogen bonding, we replaced the *N*-methyl group in peptide **1**<sub>F20(N-Me)</sub> with a *C* $\alpha$ -methyl group, thus furnishing peptide **1**<sub>F19( $\alpha$ -Me)</sub>. Peptide **1**<sub>F19( $\alpha$ -Me)</sub> crystallizes, assembling to form a triangular trimer similar to the one formed by peptide **1**<sub>F20(N-Me)</sub>. In the triangular trimer formed by peptide **1**<sub>F19( $\alpha$ -Me)</sub> all backbone NH groups are available to—and do—form intermolecular hydro-

gen bonds. Differences in  $\beta$ -sheet registration within the trimer formed by peptide  $\mathbf{1}_{F19(\alpha\text{-Me})}$  contribute to the assembly of a more compact, ball-shaped dodecamer in the crystal lattice than the dodecamer formed by peptide  $\mathbf{1}_{F20(N\text{-Me})}$ .

## RESULTS AND DISCUSSION

**Peptide Synthesis.** Peptides  $\mathbf{1}_{F20(N\text{-Me})}$ ,  $\mathbf{1}$ , and  $\mathbf{1}_{F19(\alpha\text{-Me})}$  were synthesized using standard Fmoc-based solid phase peptide synthesis (SPPS), using methods previously reported by our laboratory.<sup>23,27,28</sup> Both  $N^\alpha$ -Fmoc- $N$ -methyl- $L$ -phenylalanine and  $N^\alpha$ -Fmoc- $\alpha$ -methyl- $L$ -phenylalanine are commercially available as building blocks for SPPS. Briefly, the synthesis began by installing Fmoc-Orn(Boc)-OH onto 2-chlorotrityl chloride resin as  $^{\circ}\text{Orn}_2$ . Then for each peptide, a fragment extending from Asp<sub>23</sub> to the residue following the  $N$ - or  $\alpha$ -methylated phenylalanine was coupled by hand.<sup>29</sup> The residue following the methylated phenylalanine was double coupled using 2-(7-aza-1*H*-benzotriazole-1-yl)-1,1,3,3-tetramethyluronium hexafluorophosphate (HATU) and 1-hydroxy-7-azabenzotriazole (HOAt) as activating agents to increase coupling efficiency.<sup>30</sup> Microwave assisted SPPS, using a CEM Liberty Blue Automated Microwave Peptide Synthesizer was used to complete the linear synthesis. Following the final Fmoc deprotection, each linear peptide was cleaved from the resin with a solution of 20% 1,1,1,3,3,3-hexafluoroisopropanol (HFIP) in dichloromethane (DCM). The linear peptides were then cyclized, globally deprotected with trifluoroacetic acid (TFA), and purified by reverse-phase HPLC, furnishing each peptide as a TFA salt. Additional details and characterization data are provided in the [Supporting Information](#).

**X-ray Crystallographic Studies of Peptide  $\mathbf{1}_{F19(\alpha\text{-Me})}$ .** Peptide  $\mathbf{1}_{F19(\alpha\text{-Me})}$  afforded crystals suitable for X-ray crystallography under the same conditions previously reported for peptide  $\mathbf{1}_{F20(N\text{-Me})}$ . In contrast, peptide  $\mathbf{1}$  formed only precipitates in the 864 conditions screened. Diffraction data for crystals of peptide  $\mathbf{1}_{F19(\alpha\text{-Me})}$  were collected to 1.00 Å at the Stanford Synchrotron Radiation Lightsource. The crystallographic structure of peptide  $\mathbf{1}_{F19(\alpha\text{-Me})}$  was solved and refined in the  $F23$  space group, with the asymmetric unit comprising two monomers of peptide  $\mathbf{1}_{F19(\alpha\text{-Me})}$ . The X-ray crystallographic phases of peptide  $\mathbf{1}_{F19(\alpha\text{-Me})}$  were solved using molecular replacement with a monomer derived from a covalently stabilized homolog of peptide  $\mathbf{1}_{F20(N\text{-Me})}$  (PDB 5SUR).<sup>20</sup> [Table S1](#) summarizes the crystallographic properties, crystallization conditions, data collection, and model refinement statistics for peptide  $\mathbf{1}_{F19(\alpha\text{-Me})}$ . X-ray crystallography reveals that peptide  $\mathbf{1}_{F19(\alpha\text{-Me})}$  folds to adopt a twisted  $\beta$ -hairpin stabilized by eight intramolecular hydrogen bonds between residues 17–23 and 30–36 ([Figure 3a](#), PDB 9BI3). Peptide  $\mathbf{1}_{F19(\alpha\text{-Me})}$  assembles in the crystal lattice to form a triangular trimer stabilized by intermolecular hydrogen-bonds and hydrophobic packing ([Figure 4a](#)). Four trimers of peptide  $\mathbf{1}_{F19(\alpha\text{-Me})}$  further assemble to form a ball-shaped dodecamer ([Figure 4b](#)).

In the X-ray crystallographic structure of peptide  $\mathbf{1}_{F19(\alpha\text{-Me})}$   $C\alpha$ -methyl-Phe<sub>19</sub> adopts an extended conformation, with  $\Phi$  and  $\Psi$  angles of ca.  $-171$  and  $-161^\circ$ , respectively ([Figures 3a](#) and [S1a](#)). When plotted, the dihedral angles of the three  $C\alpha$ -methyl-Phe<sub>19</sub> residues fall at the edge of the Ramachandran map, on the very edge of the region defining  $\beta$ -strand structure. The flanking residues (Val<sub>18</sub> and Ala<sub>21</sub>) adopt more typical  $\beta$ -sheet conformations, with  $\Phi$  and  $\Psi$  angles ranging from  $-121$  to  $-136^\circ$  and  $138$  to  $161^\circ$ , respectively ([Figure S1a](#)). In comparison, residues 18–21 in peptide  $\mathbf{1}_{F20(N\text{-Me})}$  all adopt

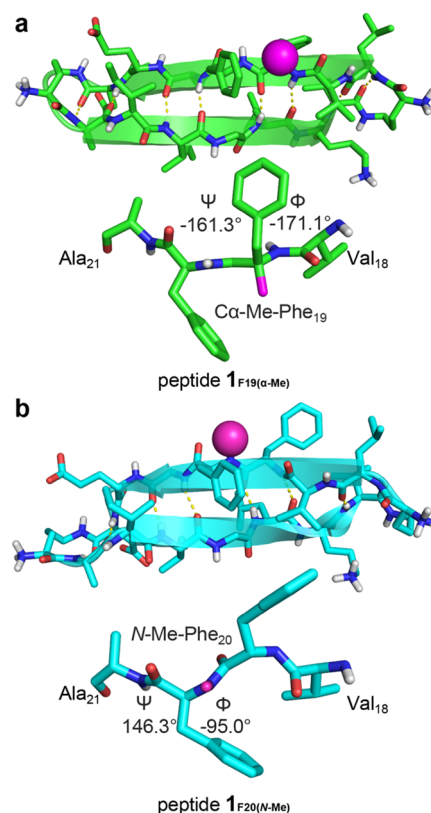


**Figure 3.** Comparison of the X-ray crystallographic structures of the twisted  $\beta$ -hairpins and  $A\beta_{18-21}$   $\beta$ -strand segments formed by (a) peptide  $\mathbf{1}_{F19(\alpha\text{-Me})}$  (PDB 9BI3) and (b) peptide  $\mathbf{1}_{F20(N\text{-Me})}$  (PDB 4NW9). The methyl groups are represented as magenta spheres.

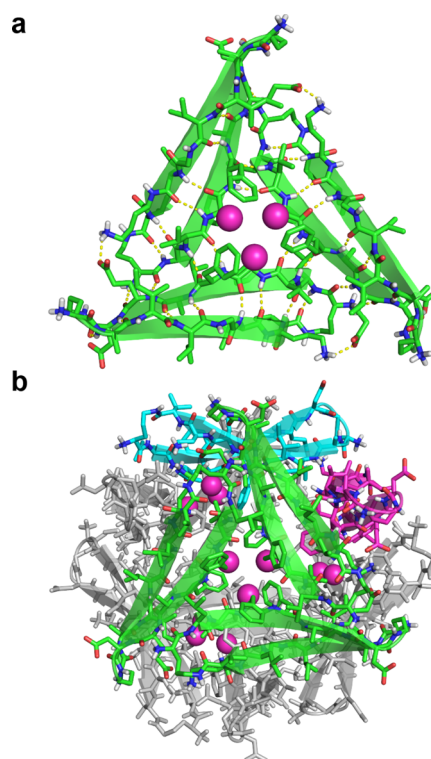


**Figure 4.** X-ray crystallographic structures of the (a) triangular trimer and (b) ball-shaped dodecamer formed by peptide  $\mathbf{1}_{F19(\alpha\text{-Me})}$ .  $\alpha$ -Methyl groups are represented as magenta spheres.



typical  $\beta$ -sheet conformations, with  $\Phi$  and  $\Psi$  angles ranging from  $-95$  to  $-148^\circ$  and  $114$  to  $157^\circ$ , respectively (Figures 3b and S1b). In turn, the  $\beta$ -strand containing  $\alpha$ -methyl-Phe<sub>19</sub> is more extended, with  $7.1$  Å between the  $\alpha$  carbons of Val<sub>18</sub> and Phe<sub>20</sub> in peptide **1**<sub>F19( $\alpha$ -Me)</sub> and  $6.5$  Å in peptide **1**<sub>F20(N-Me)</sub>. Notably, the extended  $\Phi$  and  $\Psi$  angles of the  $C\alpha$ -methyl-Phe<sub>19</sub> residue in peptide **1**<sub>F19( $\alpha$ -Me)</sub> bring the CO and NH groups of Phe<sub>19</sub> into proximity ( $2.1$  Å) and allow the formation of an intramolecular C5 hydrogen bond (Figure S2).<sup>31</sup> The steric bulk of the  $C\alpha$ -methyl group in peptide **1**<sub>F19( $\alpha$ -Me)</sub> may promote the extended backbone dihedral angles and subsequently stabilize the C5 hydrogen-bonding interaction.

Although peptides **1**<sub>F20(N-Me)</sub> and **1**<sub>F19( $\alpha$ -Me)</sub> both form triangular trimers, the trimers differ in the registration of  $\beta$ -sheet interfaces between the monomer subunits. In the trimer formed by peptide **1**<sub>F20(N-Me)</sub>, Val<sub>18</sub> pairs with Glu<sub>22</sub> (Figures S3b and S4a), while in the trimer formed by peptide **1**<sub>F19( $\alpha$ -Me)</sub>, Val<sub>18</sub> pairs with Phe<sub>20</sub> (Figures 4a and S3a). This shift in registration allows for two pairs of backbone intermolecular hydrogen bonds at the interfaces of the trimer formed by peptide **1**<sub>F19( $\alpha$ -Me)</sub>—between Val<sub>18</sub> and Phe<sub>20</sub> and  $\delta$ Orn<sub>1</sub> and Glu<sub>22</sub>. In contrast, there is only one pair of intermolecular hydrogen bonds at the interfaces of the trimer formed by peptide **1**<sub>F20(N-Me)</sub>—between Val<sub>18</sub> and Glu<sub>22</sub>. Further, the shift in  $\beta$ -sheet registration between the monomer subunits of the trimer allows for an additional intermolecular hydrogen bond between the side chains of Glu<sub>22</sub> and  $\alpha$ Orn<sub>35</sub> (Figure S3a).

Four trimers of peptide **1**<sub>F19( $\alpha$ -Me)</sub> further assemble in the crystal lattice to form a ball-shaped dodecamer (Figure 4b), similar to the dodecamer observed in the crystal lattice of peptide **1**<sub>F20(N-Me)</sub> (Figure S4b). The dodecamer formed by peptide **1**<sub>F19( $\alpha$ -Me)</sub> is more compact and spherical than the dodecamer formed by peptide **1**<sub>F20(N-Me)</sub>. The dodecamer formed by peptide **1**<sub>F19( $\alpha$ -Me)</sub> is further differentiated by the presence of additional backbone hydrogen bonds at the edges of each trimer—between Ile<sub>31</sub> and Gly<sub>30</sub> and  $\delta$ Orn<sub>2</sub> and  $\alpha$ Orn<sub>35</sub>, forming an additional type of trimer (Figure 5a). The dodecamer may also be thought of as containing four additional trimers formed at the interfaces of the primary triangular trimers (Figure 5b). The additional trimers formed by peptide **1**<sub>F19( $\alpha$ -Me)</sub> are as closely packed and hydrogen bonded as the primary triangular trimers. The greater hydrogen bonding and more compact assemblies formed by peptide **1**<sub>F19( $\alpha$ -Me)</sub> suggest that  $\alpha$ -methylation may allow the formation of more stable oligomers than those permitted by *N*-methylation.

**SDS-PAGE of Peptides 1, 1**<sub>F20(N-Me)</sub>, and **1**<sub>F19( $\alpha$ -Me)</sub>. The formation of oligomers in SDS-PAGE is a hallmark of both endogenous and synthetic full-length A $\beta$ .<sup>32–36</sup> Thus, peptide **1** exhibits a series of bands in SDS-PAGE: a strong band below the  $4.6$  kDa molecular weight marker that corresponds to the monomer and a series of weaker bands at higher molecular weights (Figure 6). In contrast, neither peptide **1**<sub>F20(N-Me)</sub> nor peptide **1**<sub>F19( $\alpha$ -Me)</sub> form oligomers in SDS-PAGE, migrating as monomer bands just below the  $4.6$  kDa molecular weight marker. The differences in self-assembly between peptide **1** and peptides **1**<sub>F20(N-Me)</sub> and **1**<sub>F19( $\alpha$ -Me)</sub> demonstrate that  $\alpha$ -methylation is an acceptable alternative to *N*-methylation in impeding solution-phase oligomerization.

## CONCLUSIONS

$\alpha$ -Methylation controls the assembly of a macrocyclic  $\beta$ -hairpin peptide derived from A $\beta$ <sub>17–36</sub>, enabling the crystallographic

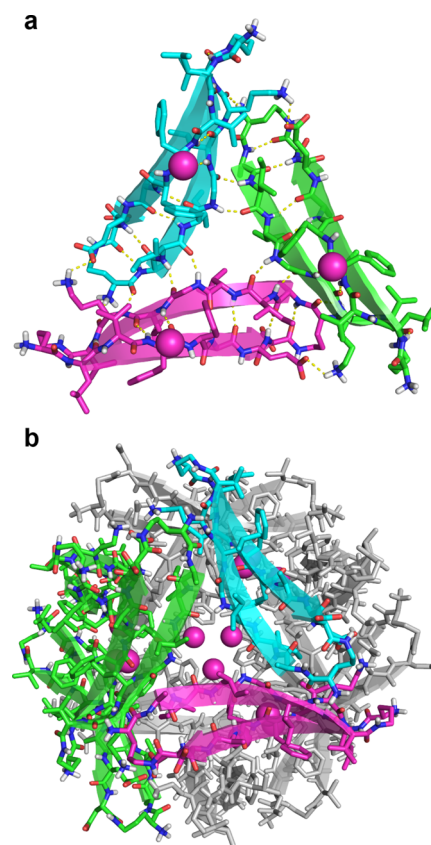


**Figure 5.** X-ray crystallographic structure of the secondary triangular trimer formed by peptide **1**<sub>F19( $\alpha$ -Me)</sub> and its assembly in the ball-shaped dodecamer. (a) View highlighting the secondary trimer formed at the interface of three triangular trimers (green, cyan, and magenta). (b) The dodecamer, which contains four of these additional trimers.

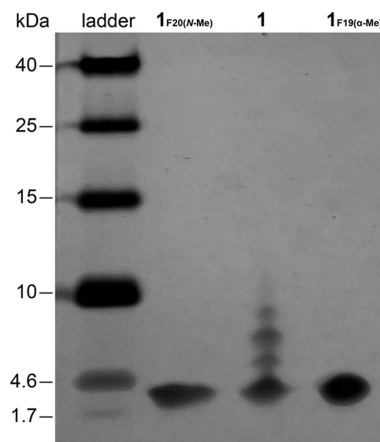


**Figure 6.** Silver stained SDS-PAGE of peptides **1**<sub>F20(N-Me)</sub>, **1**, and **1**<sub>F19( $\alpha$ -Me)</sub>. SDS-PAGE was performed in Tris buffer at pH 6.8 with 2% (w/v) SDS on a 16% poly(acrylamide gel) with  $50$   $\mu$ M solutions of peptide in each lane.

assembly of a triangular trimer and ball-shaped dodecamer. The trimer and dodecamer resemble those formed by an *N*-methylated homolog, although with subtle differences in supramolecular assembly. These differences may arise from the extended  $\beta$ -strand conformation at the site of  $\alpha$ -methylation, creating a flatter sheet structure than that formed by *N*-methylation or in a typical  $\beta$ -sheet. Alternatively, these

differences may reflect subtle differences in crystal packing, rather than inherent differences in supramolecular stability or peptide alignment.<sup>20</sup> Both  $\alpha$ -methylation and *N*-methylation permit the crystallization of a macrocyclic  $\beta$ -hairpin peptide derived from  $A\beta$  which would otherwise aggregate.  $\alpha$ -Methylation affords the attractive feature of preserving all NH hydrogen-bond donors along the peptide backbone.

Several other backbone-modification strategies have been developed to control  $A\beta$  assembly, mostly commonly by inhibiting  $A\beta$  fibrilization. Doig and co-workers have reported that *N*-methylated peptide fragments derived from  $A\beta$  inhibit  $A\beta$  fibrilization and toxicity.<sup>37,38</sup> Hammer and Garino developed peptides containing  $\alpha,\alpha$ -disubstituted amino acids that inhibit  $A\beta$  fibril formation and instead promote the formation of globular  $A\beta$  assemblies.<sup>39,40</sup> Del Valle and co-workers developed *N*-aminated amino acids that induce a  $\beta$ -strand conformation and have used  $A\beta$ -derived *N*-aminated peptides to inhibit  $A\beta$  fibrilization.<sup>41–43</sup>

$\alpha$ -Aminoisobutyric acid (Aib)—perhaps the most commonly studied  $\alpha,\alpha$ -disubstituted amino acid—is known to strongly promote helical structures and can act as a  $\beta$ -breaker by disfavoring  $\beta$ -sheet formation.<sup>44–46</sup> Although the  $\alpha$ -methyl-L-phenylalanine residue introduced here has a superficial resemblance to Aib, the bulkiness of its benzyl group promotes  $\beta$ -sheet formation. To this end, Toniolo, Lengyel, and Horne have shown that  $\alpha,\alpha$ -disubstituted amino acids with bulkier substituents can adopt extended dihedral torsions that support  $\beta$ -sheet conformations.<sup>47–52</sup> We envision that other  $\alpha$ -methylated amino acids with bulky side chains, such as  $\alpha$ -methyl-L-valine and  $\alpha$ -methyl-L-leucine, should also be useful for controlling  $\beta$ -sheet aggregation and permitting the crystallographic observation of assemblies formed by other amyloidogenic peptides.

## ■ ASSOCIATED CONTENT

### Data Availability Statement

The data underlying this study are available in the published article and its Supporting Information.

### Supporting Information

The Supporting Information is available free of charge at <https://pubs.acs.org/doi/10.1021/acs.joc.4c02344>.

HPLC and MS characterization data and X-ray crystallographic statistics for peptide  $I_{F19(\alpha-Me)}$  (PDF)

### Accession Codes

Crystallographic coordinates of peptide  $I_{F19(\alpha-Me)}$  were deposited into the Protein Data Bank (PDB) with code 9BI3.

## ■ AUTHOR INFORMATION

### Corresponding Author

James S. Nowick — Department of Chemistry, University of California, Irvine, California 92697, United States; Department of Pharmaceutical Sciences, University of California, Irvine, California 92697, United States; [orcid.org/0000-0002-2273-1029](https://orcid.org/0000-0002-2273-1029); Email: [jsnowick@uci.edu](mailto:jsnowick@uci.edu)

### Authors

Tuan D. Samdin — Department of Chemistry, University of California, Irvine, California 92697, United States; [orcid.org/0000-0003-3516-9175](https://orcid.org/0000-0003-3516-9175)

Adam G. Kreutzer — Department of Chemistry, University of California, Irvine, California 92697, United States; [orcid.org/0000-0002-9724-6298](https://orcid.org/0000-0002-9724-6298)

Victoria Sahrai — Department of Chemistry, University of California, Irvine, California 92697, United States

Michal Wierzbicki — Department of Chemistry, University of California, Irvine, California 92697, United States

Complete contact information is available at:

<https://pubs.acs.org/10.1021/acs.joc.4c02344>

### Author Contributions

T.D.S. and V.S. synthesized all peptides reported in this investigation. T.D.S. and V.S. identified and optimized crystallization conditions for peptide  $I_{F19(\alpha-Me)}$ . T.D.S. and M.W. collected X-ray diffraction data for peptide  $I_{F19(\alpha-Me)}$ . T.D.S., A.G.K., and M.W. solved and refined the crystal structure of peptide  $I_{F19(\alpha-Me)}$ . T.D.S. analyzed the structure of peptide  $I_{F19(\alpha-Me)}$  and ran the SDS-PAGE experiment. T.D.S. prepared the manuscript under the supervision of J.S.N., who provided guidance on experimental design, writing, and editing of the manuscript.

### Notes

The authors declare no competing financial interest.

## ■ ACKNOWLEDGMENTS

We thank the National Institutes of Health (NIH) National Institute on Aging (NIA) for funding (AG072587). We also thank the Stanford Synchrotron Radiation Lightsource (SSRL) Structural Molecular Biology Program (SMBP) for synchrotron data collection. The SMBP is supported in part by the DOE Office of Biological and Environmental Research, the NIH, and NIGMS. The SSRL is supported by the U.S. Department of Energy, Office of Science, Office of Basic Energy Sciences under contract no. DE-AC02-76SF00515. M.W. acknowledges the support from the Ministry of Science and Higher Education, Republic of Poland (Mobility Plus grant no. 1647/MOB/V/2017/0). T.D.S. acknowledges the support from the University of California, Irvine, for funding through the Graduate Dean's Dissertation Year Fellowship.

## ■ REFERENCES

- Walsh, D. M.; Klyubin, I.; Fadeeva, J. V.; Cullen, W. K.; Anwyl, R.; Wolfe, M. S.; Rowan, M. J.; Selkoe, D. J. Naturally Secreted Oligomers of Amyloid  $\beta$  Protein Potentially Inhibit Hippocampal Long-Term Potentiation in Vivo. *Nature* **2002**, *416* (6880), 535–539.
- Shankar, G. M.; Li, S.; Mehta, T. H.; Garcia-Munoz, A.; Shepardson, N. E.; Smith, I.; Brett, F. M.; Farrell, M. A.; Rowan, M. J.; Lemere, C. A.; Regan, C. M.; Walsh, D. M.; Sabatini, B. L.; Selkoe, D. J. Amyloid- $\beta$  Protein Dimers Isolated Directly from Alzheimer's Brains Impair Synaptic Plasticity and Memory. *Nat. Med.* **2008**, *14* (8), 837–842.
- Kreutzer, A. G.; Parrocha, C. M. T.; Haerianardakani, S.; Guaglianone, G.; Nguyen, J. T.; Diab, M. N.; Yong, W.; Perez-Rosendahl, M.; Head, E.; Nowick, J. S. Antibodies Raised Against an  $A\beta$  Oligomer Mimic Recognize Pathological Features in Alzheimer's Disease and Associated Amyloid-Disease Brain Tissue. *ACS Cent. Sci.* **2024**, *10* (1), 104–121.
- De, S.; Whiten, D. R.; Ruggeri, F. S.; Hughes, C.; Rodrigues, M.; Sideris, D. I.; Taylor, C. G.; Aprile, F. A.; Muyldermaans, S.; Knowles, T. P. J.; Vendruscolo, M.; Bryant, C.; Blennow, K.; Skoog, I.; Kern, S.; Zetterberg, H.; Klenerman, D. Soluble Aggregates Present in Cerebrospinal Fluid Change in Size and Mechanism of Toxicity during Alzheimer's Disease Progression. *Acta Neuropathol. Commun.* **2019**, *7* (1), 120.

- (5) Michaels, T. C. T.; Šarić, A.; Curk, S.; Bernfur, K.; Arosio, P.; Meisl, G.; Dear, A. J.; Cohen, S. I. A.; Dobson, C. M.; Vendruscolo, M.; Linse, S.; Knowles, T. P. J. Dynamics of Oligomer Populations Formed during the Aggregation of Alzheimer's A $\beta$ 42 Peptide. *Nat. Chem.* **2020**, *12* (5), 445–451.
- (6) Jeon, J.; Yau, W. M.; Tycko, R. Early Events in Amyloid- $\beta$  Self-Assembly Probed by Time-Resolved Solid State NMR and Light Scattering. *Nat. Commun.* **2023**, *14* (1), 2964.
- (7) Michaels, T. C. T.; Qian, D.; Šarić, A.; Vendruscolo, M.; Linse, S.; Knowles, T. P. J. Amyloid Formation as a Protein Phase Transition. *Nat. Rev. Phys.* **2023**, *5* (7), 379–397.
- (8) Rinauro, D. J.; Chiti, F.; Vendruscolo, M.; Limbocker, R. Misfolded Protein Oligomers: Mechanisms of Formation, Cytotoxic Effects, and Pharmacological Approaches against Protein Misfolding Diseases. *Mol. Neurodegener.* **2024**, *19* (1), 20.
- (9) Yu, L.; Edalji, R.; Harlan, J. E.; Holzman, T. F.; Lopez, A. P.; Labkovsky, B.; Hillen, H.; Barghorn, S.; Ebert, U.; Richardson, P. L.; Miesbauer, L.; Solomon, L.; Bartley, D.; Walter, K.; Johnson, R. W.; Hajduk, P. J.; Olejniczak, E. T. Structural Characterization of a Soluble Amyloid  $\beta$ -Peptide Oligomer. *Biochemistry* **2009**, *48* (9), 1870–1877.
- (10) Hoyer, W.; Grönwall, C.; Jonsson, A.; Ståhl, S.; Hård, T. Stabilization of a  $\beta$ -Hairpin in Monomeric Alzheimer's Amyloid- $\beta$  Peptide Inhibits Amyloid Formation. *Proc. Natl. Acad. Sci. U.S.A.* **2008**, *105* (13), 5099–5104.
- (11) Lendel, C.; Bjerring, M.; Dubnovitsky, A.; Kelly, R. T.; Filippov, A.; Antzutkin, O. N.; Nielsen, N. C.; Hård, T. A Hexameric Peptide Barrel as Building Block of Amyloid- $\beta$  Protofibrils. *Angew. Chem., Int. Ed.* **2014**, *53*, 12756–12760.
- (12) Ciudad, S.; Puig, E.; Botzanowski, T.; Meigooni, M.; Arango, A. S.; Do, J.; Mayzel, M.; Bayoumi, M.; Chaignepain, S.; Maglia, G.; Cianferani, S.; Orekhov, V.; Tajkhorshid, E.; Bardiaux, B.; Carulla, N. A $\beta$ (1–42) Tetramer and Octamer Structures Reveal Edge Conductivity Pores as a Mechanism for Membrane Damage. *Nat. Commun.* **2020**, *11* (1), 3014.
- (13) Ghosh, U.; Thurber, K. R.; Yau, W. M.; Tycko, R. Molecular Structure of a Prevalent Amyloid- $\beta$  Fibril Polymorph from Alzheimer's Disease Brain Tissue. *Proc. Natl. Acad. Sci. U.S.A.* **2021**, *118* (4), e2023089118.
- (14) Ruttenberg, S. M.; Nowick, J. S. A Turn for the Worse: A $\beta$   $\beta$ -Hairpins in Alzheimer's Disease. *Bioorg. Med. Chem.* **2024**, *105*, No. 117715.
- (15) Kreutzer, A. G.; Nowick, J. S. Elucidating the Structures of Amyloid Oligomers with Macrocyclic  $\beta$ -Hairpin Peptides: Insights into Alzheimer's Disease and Other Amyloid Diseases. *Acc. Chem. Res.* **2018**, *51*, 706–718.
- (16) Samdin, T. D.; Kreutzer, A. G.; Nowick, J. S. Exploring Amyloid Oligomers with Peptide Model Systems. *Curr. Opin. Chem. Biol.* **2021**, *64*, 106–115.
- (17) Spencer, R. K.; Li, H.; Nowick, J. S. X-Ray Crystallographic Structures of Trimers and Higher-Order Oligomeric Assemblies of a Peptide Derived from A $\beta$ <sub>17–36</sub>. *J. Am. Chem. Soc.* **2014**, *136* (15), 5595–5598.
- (18) Kreutzer, A. G.; Hamza, I. L.; Spencer, R. K.; Nowick, J. S. X-Ray Crystallographic Structures of a Trimer, Dodecamer, and Annular Pore Formed by an A $\beta$ <sub>17–36</sub>  $\beta$ -Hairpin. *J. Am. Chem. Soc.* **2016**, *138* (13), 4634–4642.
- (19) Kreutzer, A. G.; Spencer, R. K.; McKnelly, K. J.; Yoo, S.; Hamza, I. L.; Salveson, P. J.; Nowick, J. S. A Hexamer of a Peptide Derived from A $\beta$ <sub>16–36</sub>. *Biochemistry* **2017**, *56* (45), 6061–6071.
- (20) Kreutzer, A. G.; Yoo, S.; Spencer, R. K.; Nowick, J. S. Stabilization, Assembly, and Toxicity of Trimers Derived from A $\beta$ . *J. Am. Chem. Soc.* **2017**, *139* (2), 966–975.
- (21) Salveson, P. J.; Spencer, R. K.; Kreutzer, A. G.; Nowick, J. S. X-Ray Crystallographic Structure of a Compact Dodecamer from a Peptide Derived from A $\beta$ <sub>16–36</sub>. *Org. Lett.* **2017**, *19* (13), 3462–3465.
- (22) Kreutzer, A. G.; Guaglianone, G.; Yoo, S.; Parrocha, C. M. T.; Ruttenberg, S. M.; Malonis, R. J.; Tong, K.; Lin, Y.-F.; Nguyen, J. T.; Howitz, W. J.; Diab, M. N.; Hamza, I. L.; Lai, J. R.; Wysocki, V. H.; Nowick, J. S. Probing Differences Among A $\beta$  Oligomers with Two Triangular Trimers Derived from A $\beta$ . *Proc. Natl. Acad. Sci. U.S.A.* **2023**, *120* (22), e2219216120.
- (23) Samdin, T. D.; Wierzbicki, M.; Kreutzer, A. G.; Howitz, W. J.; Valenzuela, M.; Smith, A.; Sahrai, V.; Truex, N. L.; Klun, M.; Nowick, J. S. Effects of N-Terminal Residues on the Assembly of Constrained  $\beta$ -Hairpin Peptides Derived from A $\beta$ . *J. Am. Chem. Soc.* **2020**, *142* (26), 11593–11601.
- (24) Kreutzer, A. G.; Samdin, T. D.; Guaglianone, G.; Spencer, R. K.; Nowick, J. S. X-Ray Crystallography Reveals Parallel and Antiparallel  $\beta$ -Sheet Dimers of a  $\beta$ -Hairpin Derived from A $\beta$ <sub>16–36</sub> That Assemble to Form Different Tetramers. *ACS Chem. Neurosci.* **2020**, *11* (15), 2340–2347.
- (25) Ruttenberg, S. M.; Kreutzer, A. G.; Truex, N. L.; Nowick, J. S.  $\beta$ -Hairpin Alignment Alters Oligomer Formation in A $\beta$ -Derived Peptides. *Biochemistry* **2024**, *63*, 212–218.
- (26) Haerianardakani, S.; Kreutzer, A. G.; Salveson, P. J.; Samdin, T. D.; Guaglianone, G. E.; Nowick, J. S. Phenylalanine Mutation to Cyclohexylalanine Facilitates Triangular Trimer Formation by  $\beta$ -Hairpins Derived from A $\beta$ . *J. Am. Chem. Soc.* **2020**, *142*, 20708–20716.
- (27) Guaglianone, G.; Kreutzer, A. G.; Nowick, J. S. *Synthesis and Study of Macrocyclic  $\beta$ -Hairpin Peptides for Investigating Amyloid Oligomers*, 1st ed.; Elsevier Inc., 2021; Vol. 656.
- (28) Samdin, T. D.; Jones, C. R.; Guaglianone, G.; Kreutzer, A. G.; Freitas, J. A.; Wierzbicki, M.; Nowick, J. S. A  $\beta$ -Barrel-like Tetramer Formed by a  $\beta$ -Hairpin Derived from A $\beta$ . *Chem. Sci.* **2023**, *15* (1), 285–297.
- (29) Our laboratory prefers to introduce methylated residues, and the residue that follows it, by hand—however, it is not necessary to do so.
- (30) McKnelly, K. J.; Sokol, W.; Nowick, J. S. Anaphylaxis Induced by Peptide Coupling Agents: Lessons Learned from Repeated Exposure to HATU, HBTU, and HCTU. *J. Org. Chem.* **2020**, *85* (3), 1764–1768.
- (31) Newberry, R. W.; Raines, R. T. A Prevalent Intraresidue Hydrogen Bond Stabilizes Proteins. *Nat. Chem. Biol.* **2016**, *12*, 1084–1089.
- (32) Cline, E. N.; Bicca, M. A.; Viola, K. L.; Klein, W. L. The Amyloid- $\beta$  Oligomer Hypothesis: Beginning of the Third Decade. *J. Alzheimer's Dis.* **2018**, *64*, S567–S610.
- (33) Masters, C. L.; Simms, G.; Weinman, N. A.; Multhaup, G.; McDonald, B. L.; Beyreuther, K. Amyloid Plaque Core Protein in Alzheimer Disease and Down Syndrome. *Proc. Natl. Acad. Sci. U.S.A.* **1985**, *82* (12), 4245–4249.
- (34) Selkoe, D. J.; Abraham, C. R.; Podlisny, M. B.; Duffy, L. K. Isolation of Low-molecular-weight Proteins from Amyloid Plaque Fibers in Alzheimer's Disease. *J. Neurochem.* **1986**, *46* (6), 1820–1834.
- (35) Podlisny, M. B.; Ostaszewski, B. L.; Squazzo, S. L.; Koo, E. H.; Rydell, R. E.; Teplow, D. B.; Selkoe, D. J. Aggregation of Secreted Amyloid  $\beta$ -Protein into Sodium Dodecyl Sulfate-Stable Oligomers in Cell Culture. *J. Biol. Chem.* **1995**, *270*, 9564–9570.
- (36) Zhang, S.; Yoo, S.; Snyder, D. T.; Katz, B. B.; Henrickson, A.; Demeler, B.; Wysocki, V. H.; Kreutzer, A. G.; Nowick, J. S. A Disulfide-Stabilized A $\beta$  That Forms Dimers but Does Not Form Fibrils. *Biochemistry* **2022**, *61* (4), 252–264.
- (37) Hughes, E.; Burke, R. M.; Doig, A. J. Inhibition of Toxicity in the  $\beta$ -Amyloid Peptide Fragment  $\beta$ -(25–35) Using N-Methylated Derivatives. A General Strategy to Prevent Amyloid Formation. *J. Biol. Chem.* **2000**, *275* (33), 25109–25115.
- (38) Kokkoni, N.; Stott, K.; Amijee, H.; Mason, J. M.; Doig, A. J. N-Methylated Peptide Inhibitors of  $\beta$ -Amyloid Aggregation and Toxicity. Optimization of the Inhibitor Structure. *Biochemistry* **2006**, *45* (32), 9906–9918.
- (39) Etienne, M. A.; Aucoin, J. P.; Fu, Y.; McCarley, R. L.; Hammer, R. P. Stoichiometric Inhibition of Amyloid  $\beta$ -Protein Aggregation with Peptides Containing Alternating  $\alpha,\alpha$ -Disubstituted Amino Acids. *J. Am. Chem. Soc.* **2006**, *128* (11), 3522–3523.



(40) Bett, C. K.; Ngunjiri, J. N.; Serem, W. K.; Fontenot, K. R.; Hammer, R. P.; McCarley, R. L.; Garno, J. C. Structure-Activity Relationships in Peptide Modulators of  $\beta$ -Amyloid Protein Aggregation: Variation in  $\alpha,\alpha$ -Disubstitution Results in Altered Aggregate Size and Morphology. *ACS Chem. Neurosci.* **2010**, *1* (9), 608–626.

(41) Sarnowski, M. P.; Kang, C. W.; Elbatrawi, Y. M.; Wojtas, L.; Del Valle, J. R. Peptide N-Amination Supports  $\beta$ -Sheet Conformations. *Angew. Chem., Int. Ed.* **2017**, *56* (8), 2083–2086.

(42) Sarnowski, M. P.; Pedretty, K. P.; Giddings, N.; Woodcock, H. L.; Del Valle, J. R. Synthesis and  $\beta$ -Sheet Propensity of Constrained N-Amino Peptides. *Bioorg. Med. Chem.* **2018**, *26* (6), 1162–1166.

(43) Tillett, K. C.; Del Valle, J. R. N -Amino Peptide Scanning Reveals Inhibitors of A $\beta$ 42 Aggregation. *RSC Adv.* **2020**, *10* (24), 14331–14336.

(44) O'Neil, K. T.; DeGrado, W. F. A Thermodynamic Scale for the Helix-Forming Tendencies of the Commonly Occurring Amino Acids. *Science* **1990**, *250* (4981), 646–651.

(45) Karle, I. L.; Balaram, P. Structural Characteristics of  $\alpha$ -Helical Peptide Molecules Containing Aib Residues. *Biochemistry* **1990**, *29* (29), 6747–6756.

(46) Venkatraman, J.; Shankaramma, S. C.; Balaram, P. Design of Folded Peptides. *Chem. Rev.* **2001**, *101* (10), 3131–3152.

(47) Toniolo, C.; Crisma, M.; Formaggio, F.; Peggion, C. Control of Peptide Conformation by the Thorpe-Ingold Effect ( $C\alpha$ -Tetrasubstitution). *Pept. Sci.: Orig. Res. Biomol.* **2001**, *60* (6), 396–419.

(48) Peggion, C.; Moretto, A.; Formaggio, F.; Crisma, M.; Toniolo, C. Multiple, Consecutive, Fully-Extended 2.05-Helix Peptide Conformation. *Biopolymers* **2013**, *100* (6), 621–636.

(49) Karnes, M. A.; Schettler, S. L.; Werner, H. M.; Kurz, A. F.; Horne, W. S.; Lengyel, G. A. Thermodynamic and Structural Impact of  $\alpha,\alpha$ -Dialkylated Residue Incorporation in a  $\beta$ -Hairpin Peptide. *Org. Lett.* **2016**, *18* (15), 3902–3905.

(50) Heath, S. L.; Horne, W. S.; Lengyel, G. A. Effects of Chirality and Side Chain Length in  $C\alpha,\alpha$ -Dialkylated Residues on  $\beta$ -Hairpin Peptide Folded Structure and Stability. *Org. Biomol. Chem.* **2023**, *21*, 6320–6324.

(51) Lengyel, G. A.; Reinert, Z. E.; Griffith, B. D.; Horne, W. S. Comparison of Backbone Modification in Protein  $\beta$ -Sheets by A $\rightarrow$  $\gamma$  Residue Replacement and  $\alpha$ -Residue Methylation. *Org. Biomol. Chem.* **2014**, *12* (29), 5375–5381.

(52) George, K. L.; Horne, W. S. Foldamer Tertiary Structure through Sequence-Guided Protein Backbone Alteration. *Acc. Chem. Res.* **2018**, *51* (5), 1220–1228.